Langevin Dynamic Simulations for Polymer Conformation in Shear and Turbulent Flows

Lauren Farndell[1, a)], Lee Mortimer[1, b)], and Michael Fairweather[1,c)]

Author Affiliations
[1]*School of Chemical and Process Engineering*
University of Leeds
Woodhouse Lane, Leeds, LS2 9JT
UNITED KINGDOM

Author Emails
[a)] *pm19lf@leeds.ac.uk*
[b)] *l.f.mortimer@leeds.ac.uk*
[c)] *m.fairweather@leeds.ac.uk*

Abstract. A novel potential-based computational approach to modeling polymer dynamics within shear and turbulent flows is presented and demonstrated to aid understanding of the use of polymeric flocculants for nuclear waste treatment. The research investigates the effect of varying shear rates on polymer conformation within turbulent shear flows, to identify ideal shear rates for flocculation treatment. Direct numerical simulation is used to simulate the continuous phase, alongside modeling of the polymeric phase using Langevin dynamics and the finitely extensible nonlinear elastic bead-spring model. The Kratky-Porod bending potential and steric monomer interactions are also included in the calculations to account for more realistic conformation conditions. Following validation using experimental data from existing literature, the relationship between polymer conformation properties, including the mean radius of gyration, end-to-end distance, and increasing shear rate is investigated for wall-normal regions within Re_τ= 180 and Re_τ= 300 turbulent channel flows. It is demonstrated that polymer extension generally increases with shear rate and turbulence level; however, the largest extensions were observed at the lowest Reynolds number, which is likely caused by more pronounced tumbling mechanisms and drag reduction effects at higher turbulence. To aid flocculation, it is recommended that a low-to-medium shear rate should be used for the treatment of particle-laden flows, to promote polymer extension, and to increase the collision cross section with the particulate phase.

Key-Words. Multiphase flows, polymeric flows, Langevin dynamics, polymer conformation, shear flows, turbulence.

INTRODUCTION

Nuclear waste clean-up stands as one of the most pressing challenges facing the UK nuclear decommissioning effort at present. One proposed treatment of particle-laden slurry flows at waste disposal and reprocessing sites is the addition of small concentrations of polymer additives to aid in the flocculation and agglomeration of particles, in an effort to separate suspended solids from the liquid flow which can then be treated using other conventional techniques [1]. This would result in cost savings as well as reduced timescales for the overall treatment of the waste and would lower the chance of accidental release or contamination of the environment. That said, polymer dynamics are very complex, with dynamics occurring on a multitude of scales from the bulk flocculation scale down to the molecular scale. Furthermore, there are limited studies available in the literature surrounding their behaviour in shear or turbulent flows, which plays an important role in their subsequent flocculation dynamics. Understanding of polymer activity within shear and turbulent flows is therefore essential to underpin the foundational knowledge needed before formulation of any treatment strategy.

Langevin dynamics is used to study molecular systems using simplified models, with computational methodologies now able to predict and assess polymeric flow over time [2]. Previous computational studies provide several conclusions on the effect of polymers on turbulent flow. This includes effects in the buffer layer, including a reduction in streamwise vorticity fluctuations and increased spacing between turbulent streaks, suggesting turbulence suppression [3]. Further findings include that the extent of drag reduction is dependent on the maximum average chain

extensibility and the friction Weissenberg number, *Wi*, due to the polymers suppressing turbulent eddies within the buffer layer [4].

Polymer conformation studies tend to suggest that greater shear rates lead to larger polymer extensions and greater streamwise extension within a turbulent channel [5]. Chain extension also increases from the bulk flow in the channel to the viscous sublayer. However, chain extension caused by turbulence has been found to be greatest in the buffer layer due to stronger velocity gradients. Turbulence structures then lead to greater polymer extension within this region [5], [6]. The existing literature provides conclusions surrounding polymer conformation for wall-normal regions, but is yet to directly compare the effect of increasing Reynolds number, which the present work aims to understand.

The present work aims to use Langevin dynamic simulations to develop understanding underpinning polymer conformation within shear flows, as well as to determine how varying shear rates can affect polymeric dynamic properties. A high-fidelity computational-based methodology has been selected in order to explore deeper into the fundamental hydrodynamic processes, as complex experimental methodologies would be required if the study was undertaken physically. Following the introduction of the governing equations, the simulation environment used in the following work is validated against existing literature results through calculation of the radius of gyration (R_g), end-to-end distance (R_0), and fractional extension under quiescent and simple shear conditions. With the aim of understanding polymer conformation under turbulent flows, DNS is used to calculate R_g and R_0 distributions for $Re_\tau = 180$ and $Re_\tau = 300$, over the entire turbulent channel flow, as well as for specific wall-normal regions. Comparison of polymer conformation properties for increasing Reynolds number and varying regions using a potential-based finitely extensible nonlinear elastic (FENE) chain model is a novel approach and is yet to be widely adopted in the literature. Conclusions may then be drawn relating polymer conformations under varying shear rates to possible flocculation treatments for contaminated multiphase flows.

PROBLEM FORMULATION

A novel potential-based approach using Langevin dynamics and the finitely extensible nonlinear elastic bead-spring model is used. This model assumes that each polymer is modeled as macromolecular chains of interacting bead-spring components, where each monomer bead is subject to a nonlinear elastic force, increasing with polymer extension.

A force-balance governing equation which models the position vector of each bead is used [2]:

$$m_b \frac{d^2 \boldsymbol{r_i}}{dt^2} = -\nabla V_i - \xi \left(\frac{d(\boldsymbol{r_i})}{dt} - \boldsymbol{u}_{F,i} \right) + \sqrt{2 k_B T \xi} \eta_i(t), \tag{1}$$

where m_b is the monomer bead mass, $\boldsymbol{r}_i$ is the position vector of bead i, t is time, V_i represents the interaction potentials, ξ is the drag coefficient of each bead given by Stokes' law, $\boldsymbol{u}_{F,i}$ is the interpolated fluid velocity vector, k_B is the Boltzmann constant, T is the ambient temperature and η_i represents the Brownian noise. This may be converted to non-dimensional units (denoted by the symbol $*$) using a constant monomer bead diameter σ_b. Time is non-dimensionalized using the Brownian bead timescale $t_b^* = \sqrt{m_b \sigma_b / k_B T}$. The diffusion coefficient $D = k_B T / \xi$ may also be substituted and Eq. (1) can then be re-written in non-dimensional units:

$$\frac{d^2 \boldsymbol{r}_i^*}{dt^{*2}} = -\nabla V_i^* - \frac{1}{D} \left(\frac{d(\boldsymbol{r}_i^*)}{dt^*} - \boldsymbol{u}_{F,i}^* \right) + \sqrt{\frac{2}{D}} \eta_i^*(t^*). \tag{2}$$

The interaction potential is where the FENE bead and spring model is utilized, alongside any other interactions to be modeled. The overall interaction potential is given as:

$$V_i^* = V_{i,FENE}^* + V_{i,B}^* + V_{i,WCA}^* + V_{WALL}^*. \tag{3}$$

Here, $V_{i,FENE}^*$ is the FENE bead-spring potential, used to represent the flexible bonds between a monomer bead and its neighbours:

$$V^*_{i,FENE}(\boldsymbol{r}^*_{i,i\pm1}) = -\frac{K^*_{FENE}R^{*2}_0}{2}\ln[1-(\frac{\boldsymbol{r}^*_{i,i\pm1}}{R^*_0})^2], \tag{4}$$

where $\boldsymbol{r}^*_{i,i\pm1}$ is the bead separation ($\boldsymbol{r}^*_{i,i\pm1} = |\boldsymbol{r}^*_{i\pm1} - \boldsymbol{r}^*_i|$), K^*_{FENE} is the non-dimensional FENE energy scale and R^*_0 is the maximum FENE bond length. The Kratky-Porod bending potential represents polymer bending rigidity:

$$V^*_{i,B} = K^*_{BEND}[1 + cos(\theta_i)], \tag{5}$$

where K^*_{BEND} is the bending rigidity potential strength and θ_i is the angle between two neighbouring separation vectors, i.e. $\theta_i = cos^{-1}(\hat{\boldsymbol{n}}_{\boldsymbol{i+1}}.\hat{\boldsymbol{n}}_{\boldsymbol{i}})$ with $\hat{\boldsymbol{n}}_{\boldsymbol{i}} = (\boldsymbol{r}^*_{\boldsymbol{i}} - \boldsymbol{r}^*_{\boldsymbol{i+1}})/|\boldsymbol{r}^*_{\boldsymbol{i}} - \boldsymbol{r}^*_{\boldsymbol{i+1}}|$. The Weeks-Chandler-Anderson (WCA) potential is used to represent steric interactions between each of the monomer beads:

$$V^*_{i,WCA} = 1 + 4\left[\left(\frac{\sigma}{\boldsymbol{r}_{ij}}\right)^{12} - \left(\frac{\sigma}{\boldsymbol{r}_{ij}}\right)^{6}\right], \tag{6}$$

with r_{ij} the distance between monomer i and monomer j. Finally, a potential for the wall is also included, but only when the monomer position exceeds the impenetrable domain boundaries:

$$V^*_{WALL}(\delta^*) = 10\delta^{*2}. \tag{7}$$

The domain in the turbulent channel case, shown in Fig. 1, is a $0.28m \times 0.04m \times 0.12m$ dimensional turbulent channel with periodic conditions in the streamwise (x) and spanwise (z) directions, and no-slip conditions at either limit of the wall-normal direction (y). The direct numerical simulation (DNS) solver, Nek5000, was used to generate the continuous phase solution [5].

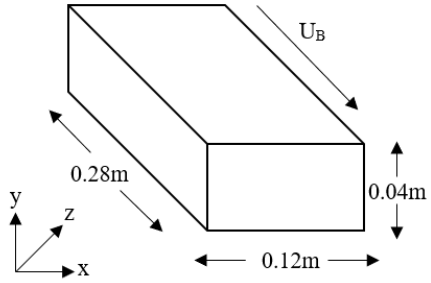

FIGURE 1. Domain geometry for the Re_τ =180, 300 turbulent channel flow.

The constant flow rate was maintained by a pressure gradient across the channel:

$$\frac{\partial p^*}{\partial x^*} = \left(\frac{Re_\tau}{Re_B}\right)^2, \tag{8}$$

where $\frac{\partial p^*}{\partial x^*}$ is the pressure gradient and Re_B is the bulk Reynolds number. A chaotic initial profile is used to ensure turbulence within the channel. A summary of the channel simulation parameters is given in Table 1.

TABLE 1. DNS Turbulent Channel Parameters.

Runs	**1**	**2**
Re_τ	180	300
Re_B	2800	4900
$E_x \times E_y \times E_z$	$27 \times 18 \times 23$	
$L_x \times L_y \times L_z$	$0.28 \times 0.04 \times 0.12$	

Langevin dynamics simulations were performed concurrently with the DNS, using spectral interpolation to obtain the fluid velocity at the position of the monomer beads.

RESULTS AND DISCUSSION

Validation of the Simulation Environment

Preliminary polymer conformation results in both quiescent conditions and shear flows were predicted from Langevin dynamic simulations, with polymer properties matching previous experimental studies of DNA [7]. Polymeric properties are given in Table 2 for λ-phage DNA. This type of polymer was selected for the current work due to the number of validation studies published within the literature, ensuring an accurate methodology was employed for the novel simulations presented in this study.

TABLE 2. Polymeric properties of λ-phage DNA.

Property	λ-phage DNA
Contour Length (μm)	21
Persistence Length	0.066
Effective Persistence Length	0.082
Bead Radius (μm)	0.0693

The resulting polymer conformation predictions were used to validate the methodology employed in the remainder of the study. Time-averaged plots are presented in Fig. 2 for the ensemble-averaged end-to-end chain distance (R_0) and the radius of gyration (R_g). These were calculated for 100,000 10-bead DNA polymer chains under quiescent conditions, demonstrating the fluctuation of each value against time, and compared against the mean experimentally measured value. It is evident that after an initial transient period of around 1s, the simulations correctly predict end-to-end distances and radii of gyration very close to experimental values [7].

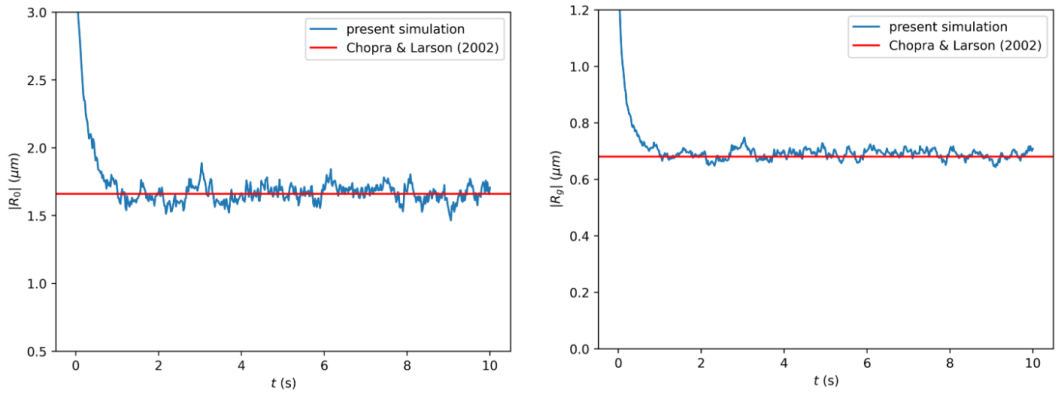

(a) (b)

FIGURE 2. Temporal evolution of the mean value of R_0 (a) and R_g (b) for polymer ensemble compared to experimental results [7].

The effect of shear rate on polymer conformation dynamics was also considered for the validation. Here, the magnitude of the shear rate is represented by the Weissenberg number. As Wi increases, the shear across the polymer chain causes the physical distance between each bead in the chain to grow, leading to stretching behavior. This is also known as the fractional extension and is illustrated in Fig. 3, which compares the probability distribution function of fractional extension against experimental observations [8]. Good agreement is obtained between the current simulation and the validation data.

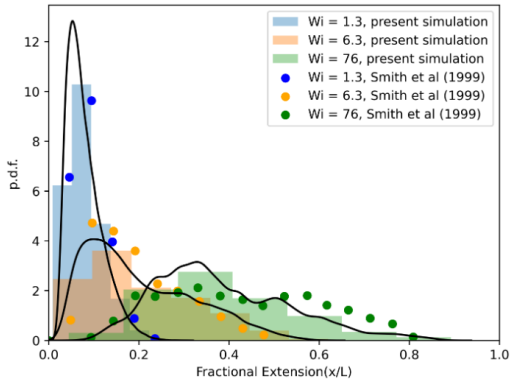

FIGURE 3. Effect of Wi number on the probability distribution function of fractional extension, x/L. Comparisons are made with simulation results. [8].

Prior to the addition of polymers, the turbulent channel flow environment was validated to ensure turbulent flow conditions had been reached and statistically stationary averaged flow profiles were observed. The channel environment was selected as it is a simple geometry for the analysis of polymeric properties under turbulent conditions, and wall-proximity-dependent phenomena such as the effect of the local turbulence kinetic energy on conformation properties could be studied. There is also extensive research surrounding simulations in turbulent channels, including at $Re_\tau = 180$ [5], [9].

Turbulent channel flow simulations in the absence of a polymeric phase were first performed for shear Reynolds numbers $Re_\tau = 180$ and 300 to examine near-wall flow dynamics. An instantaneous snapshot depicting the velocity magnitude in the $x - y$ plane is presented in Fig. 4. The velocity magnitude demonstrates turbulent structures across various regions of the channel, depicting turbulent flow.

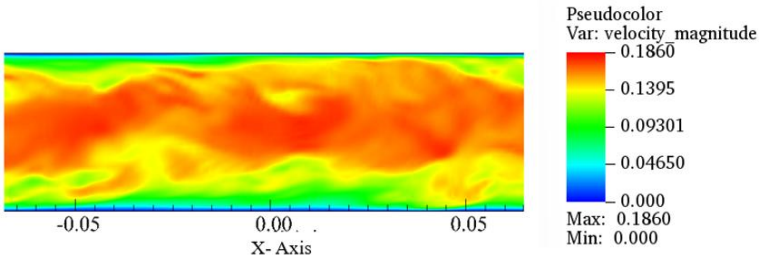

FIGURE 4. Instantaneous velocity magnitude pseudocolor plot of $x - y$ plane for turbulent channel flow at Re_τ =180.

To validate the predictions quantitatively, the mean streamwise fluid velocity and root-mean-square (RMS) velocity fluctuation profiles were plotted against the wall-normal (y) position and compared to the existing published DNS database [9]. The profiles for $Re_\tau = 180$ are presented in Fig. 5.

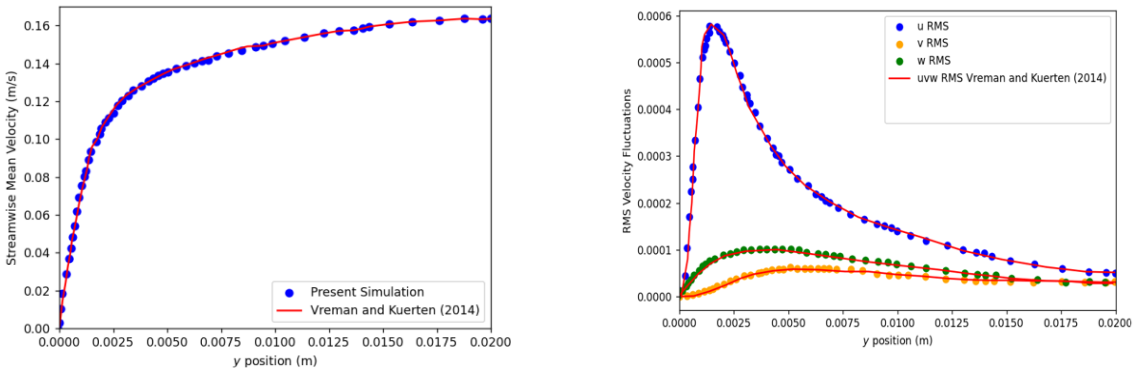

(a) (b)

FIGURE 5. Mean streamwise velocity profile (a) and RMS velocity fluctuations (b) for turbulent channel flow at $Re_\tau = 180$.

The Re_τ = 180 mean streamwise velocity and RMS velocity fluctuations are compared against the DNS result database to assess the accuracy of mean velocity and turbulence statistic predictions. As can be seen in Fig. 5, current results fit closely with those given in the validation database, indicating the turbulent flow field has been accurately created. The maximum streamwise velocity is seen at 0.17 m s^{-1} at a y position of 0.02m, and the greatest velocity fluctuation is seen in the streamwise direction at 0.0006 m s^{-1}. The current predictions using Nek5000 exhibit good agreement with the validation results, demonstrating that the turbulent flow field is accurate. Following this validation DNA polymers were injected into the turbulent channel simulations.

Polymer-laden Turbulent Channel Flows

The polymer conformation quantities, R_0 and R_g, were calculated for the DNA polymers in the Re_τ = 180 and 300 turbulent channel flows. Their distributions throughout the entire channel are presented in Fig 6. Quantitative mean values from each distribution are also provided in Table 3.

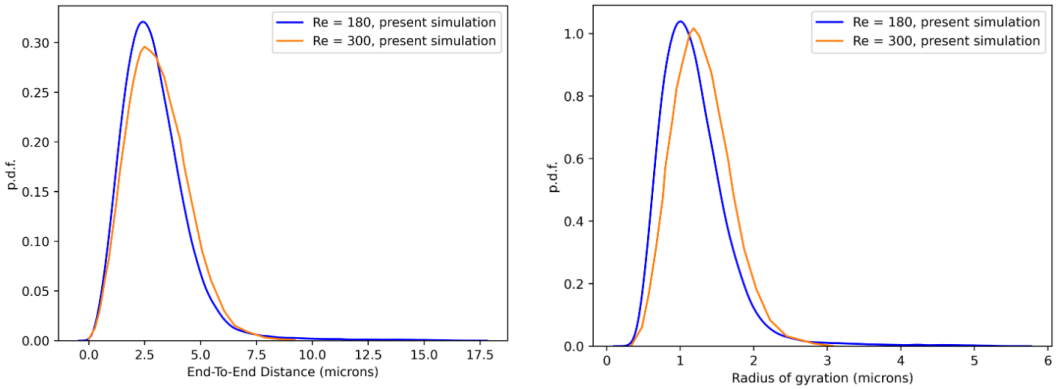

(a) (b)

FIGURE 6: R_0 distributions (a) and R_g distributions (b) for polymer confirmations in turbulent channel flows at Re_τ = 180 and 300.

TABLE 3. Polymer conformation mean values.

Re_τ	Quiescent	180	300
R_0 (μm)	1.66	2.95	3.09
R_g (μm)	0.68	1.20	1.31

When comparing the two Reynolds numbers, an overall increase in end-to-end distance and radius of gyration is observed. These properties greatly increase when the polymers are placed in the channel flow, compared to their values under quiescent conditions, and continue to increase with Re_τ. The effect of turbulence on the conformation properties is due to increases in shear across the polymer chain, leading to greater stretching. These results are hence expected when considering the forces acting on the polymer; the shear rate in the turbulent regions is higher with increasing Reynolds number and therefore, increasing turbulence. As the shear forces increase, the polymer is extended and observations of instantaneous conformation configurations (not presented here) demonstrated that most polymers in high shear regions close to the wall are uncoiled. These results are in line with those seen in the literature [7], [8], as well as both the quiescent and simple shear results present within this study.

To examine the effect of the various shear rates across the turbulent channel flow on conformation properties, R_0 and R_g were sampled within the various wall-normal regions. These are the viscous sublayer (vs), the buffer layer (bl), the log-law layer (ll), and the bulk flow (bf). Table 4 demonstrates the boundary conditions of each region.

TABLE 4. y position for each turbulent flow region.

Region	Y(Channel Centre = 0)	
	Start	**End**
Bulk Flow	0	0.016
Log-law	0.016x	0.0169
Buffer Layer	0.0169	0.0195
Viscous Sublayer	0.0195	0.02

The effect of Reynolds number is also compared, considering p.d.f.s for both $Re_\tau = 180$ and 300. These distributions are presented in Figs. 7 & 8. Quantitative mean values are provided in Table 5.

TABLE 5. Conformation properties of polymers based on channel flow region and shear Reynolds number.

Region	R_0		R_g	
	180	**300**	**180**	**300**
Viscous Sublayer	5.35	4.06	2.06	1.68
Buffer Layer	3.64	3.60	1.45	1.49
Log-law	2.89	3.13	1.18	1.32
Bulk Flow	2.76	3.01	1.13	1.28

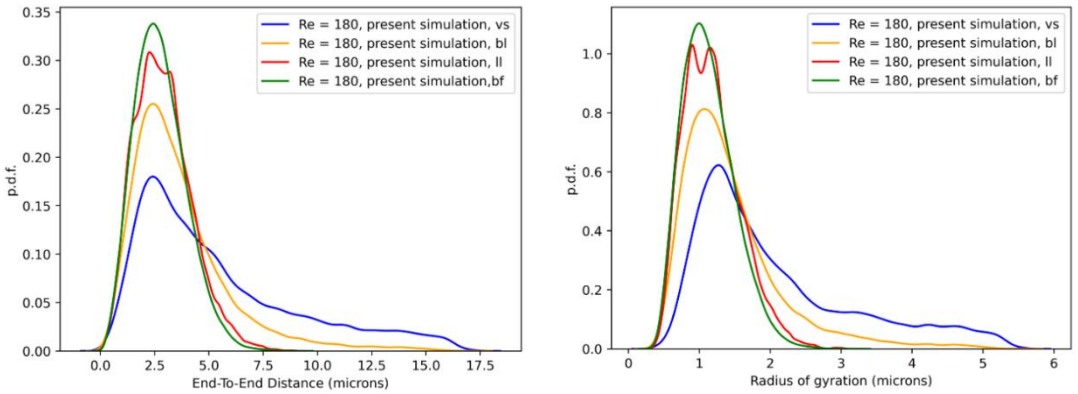

(a) (b)

FIGURE 7. Probability distribution functions of conformation property, R_0 (a) and R_g (b).The effect of the channel flow region is demonstrated at $Re_\tau = 180$.

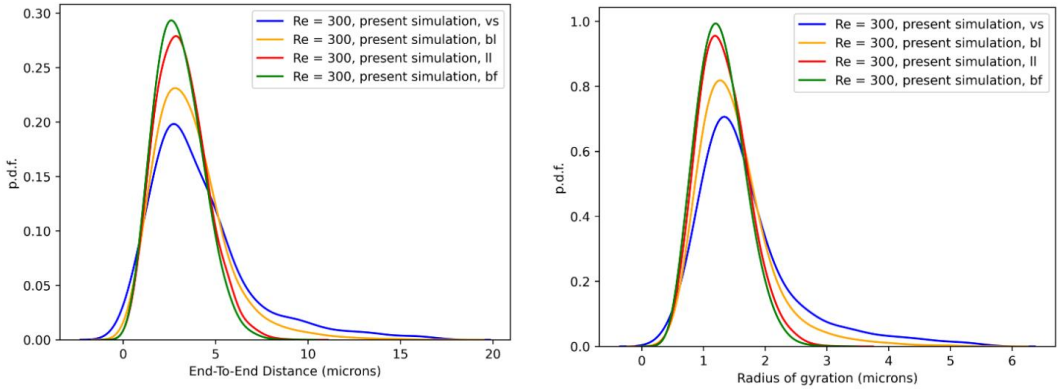

(a) (b)

FIGURE 8. Probability distribution functions of conformation property, R_0 (a) and R_g(b). The effect of the channel flow region is demonstrated at $Re_\tau = 300$.

As expected, as the shear rate within each channel increases, moving from the center of the channel to the wall, the polymeric conformation metrics increase due to the increased shear force acting on each polymer. The largest end-to-end distance and radius of gyration values are seen in the viscous sublayer, and the smallest values recorded in the bulk flow for both the $Re_\tau = 180$ and $Re_\tau = 300$ channel flows, as can be seen in Table 5. This is reflected in results in the literature [5], [6] where the largest polymer extensions are also observed in the viscous sublayer and the buffer layer, due to the increased shear force acting on each polymer within these regions.

However, within the viscous sublayer and almost all of the buffer layer, conformation property values at $Re_\tau = 180$ exceed those at $Re_\tau = 300$, despite the increase in shear rate. This is unexpected, in line with previous conclusions surrounding the positive relationship between increasing shear rate and greater polymer extension. The buffer layer properties also resemble much closer to those calculated in the viscous sublayer.

These polymer conformation metric results are thought to be due to turbulence within the flow, leading to mechanisms resulting in polymer extension. Previous literature results have observed similar results, with the dominant turbulent mechanisms such as sweeps and ejections mainly occurring beyond the viscous sublayer, leading to longer extensions in these regions [5], [6]. In regions of increased turbulence, greater tumbling mechanisms have also been observed, which acts to reduce the extension of the polymers [7]. It has also been recognized that when the bulk Reynolds number is less than 5,000 ($Re_B = 2800$ for $Re_\tau = 180$) a fully developed log-law layer is not produced, which may affect turbulence interaction dynamics in the entirety of the near-wall region [10]. It is therefore recognized that the greatest chain extension due to shear rate occurs in the viscous sublayer, whereas extension due to turbulent mechanisms is greatest in the buffer layer.

It should also be noted that the number of polymers within each wall-normal region increases from the viscous sublayer to the bulk flow, indicated by the shorter p.d.f. peaks in Figs. 7 and 8. Therefore, extension values recorded in the viscous sublayer and buffer layer are averaged over fewer polymers, resulting in more extreme extensions having a larger impact on the average end-to-end distance and radius of gyration value. The mechanisms present in the buffer layer, and the turbulent boundary layer as a whole, and the underlying reasons behind their impact on polymer conformation properties are still elusive and require further investigation.

Increasing polymer extension aids flocculation as it increases their collision cross-sections with suspended particles. Polymers are also more likely to form longer tails, and further act as bridges between particles and polymers [11]. However, only a minor increase in polymer extension is seen from $Re_\tau = 180$ to $Re_\tau = 300$. Therefore, industries considering wastewater treatment through agglomeration of particles using polymer additives should evaluate whether the increase in turbulence and shear rate to generate polymer extension is actually beneficial, compared to other effects increased shear may have on the flocculation mechanism, such as break-up and degradation of flocculants at high shear rates [12], [13].

Limitations of the present work include the incomplete quantitative validation of polymer conformation metrics in each wall-normal region, due to a lack of published studies in this area. The methodology utilized throughout the current study has been quantitatively validated for quiescent and simple shear conditions; however, the novel approach to the simulation of wall-normal regions means only qualitative comparison to the existing literature is possible, although this compares well leading to confidence in the presented results. Also, in this study, only two turbulent channel simulations are compared. This should be expanded upon to ensure the highlighted relationships between polymer extensions, shear rate, and turbulent fluctuations are reflected at higher Reynolds numbers.

CONCLUSIONS

The relationship between polymer conformation properties and shear rate, representative of turbulent regions, is presented for both $Re_\tau = 180$ and 300 turbulent channel flows, with the aim of understanding how polymer additives in shear and turbulent flows may most efficiently be used to induce flocculation of particles for slurry flow treatment. Modeling of the polymeric phase was achieved using the FENE bead-spring model and a potential-based Langevin dynamics simulation, with direct numerical simulation used to predict the continuous phase.

Initially, setup and validation of the simulation environment were completed for the polymer chains, as well as the turbulent channel flow. This was achieved through the simulation of DNA polymers under quiescent and simple shear conditions, comparing calculated R_g and R_0 values against those observed in both computational and experimental studies. Streamwise mean velocity and RMS velocity fluctuation profiles were also validated for the turbulent channel flow at $Re_\tau = 180$. Very good agreement was exhibited in each instance indicating high accuracy in the simulation methodology and generating confidence in the novel results.

Simulations of DNA polymers in turbulent channel flow for differing Re_τ were performed using DNS. Averaged across the wall-normal direction in each channel, it was found that both R_0 and R_g increased with higher turbulence,

indicating longer polymer extensions due to the increased shear rates present in the $Re_\tau = 300$ flow, in-line with recent literature observations. However, this relationship was not fully produced when comparing the individual turbulent regions, with the largest extension values present at $Re_\tau = 180$ rather than $Re_\tau = 300$. Possible conclusions include that tumbling mechanisms seen at higher Re_τ numbers, especially in the buffer layer where turbulence dominates, may impact the conformities by reducing both conformation metrics. The literature surrounding specific mechanisms of polymer-fluid interaction in turbulent regions in wall-bounded flow is limited and it is recommended that these phenomena be studied further.

For particle-laden waste flows, it is recommended that a low to medium shear rate should be used alongside polymer additives to ensure successful flocculation. Shear rates should be high enough to induce polymer tails and greater polymer extension, but not so high they produce detrimental effects to the flocculation mechanism. It is suggested that further investigation should be undertaken into turbulent mechanisms in the viscous sublayer and buffer layer, following polymer addition. The research could also be expanded by modeling larger shear Reynolds numbers to ensure polymer conformation trends recognized in the current study are also present within channels with higher levels of turbulence.

ACKNOWLEDGEMENTS

Lauren Farndell carried out the simulations, performed the analysis, and wrote the first draft of the article. Lee Mortimer assisted in supervision of the project, wrote the Langevin dynamics code, aided with setup and completion of simulations, and proofread/edited the final article. Michael Fairweather supervised the project, obtained the funding and proofread/edited the final article.

The authors are grateful to the UK Engineering and Physical Sciences Research Council for funding through the TRANSCEND (Transformative Science and Engineering for Nuclear Decommissioning) project (EP/S01019X/1), and Sellafield Ltd. for funding from the University of Leeds-Sellafield Ltd, Centre of Expertise for Sludge (Particulates & Fluids).

Conflict of Interest

The authors have no conflicts of interest to declare that are relevant to the content of this article

REFERENCES

1. A. P. G. Lockwood, J. Peakall, N. J. Warren, G. Randall, M. Barnes, D. Harbottle and T. N. Hunter, Structure and sedimentation characterisation of sheared Mg(OH)2 suspensions flocculated with anionic polymers, Chem. Eng. Sci. **231**, 116274 (2021). 10.1016/j.ces.2020.116274
2. H. Ottinger, Stochastic Processes in Polymeric Fluids: Tools and Examples for Developing Simulation Algorithms, Springer-Verlag, Berlin and Heidelberg, (2012).
3. R. Sureshkumar, A. N. Beris and R. A. Handler, Direct numerical simulation of the turbulent channel flow of a polymer solution, Phys. Fluids 9, 743–755 (1997). 10.1063/1.869229
4. C. D. Dimitropoulos, R. Sureshkumar and A. N. Beris, Direct numerical simulation of viscoelastic turbulent channel flow exhibiting drag reduction: effect of the variation of rheological parameters, J. Non-Newton. Fluid Mech. 79, 433–468 (1998). 10.1016/S0377-0257(98)00115-3
5. L. F. Mortimer and M. Fairweather, Prediction of polymer extension, drag reduction, and vortex interaction in direct numerical simulation of turbulent channel flows, Phys. Fluids **34**, 073318 (2022). 10.1063/5.0094978
6. V. K. Gupta, R. Sureshkumar and B. Khomami, Polymer chain dynamics in Newtonian and viscoelastic turbulent channel flows, Phys. Fluids 16, 1546–1566 (2004). 10.1063/1.1687415
7. M. Chopra and R. G. Larson, Brownian dynamics simulations of isolated polymer molecules in shear flow near adsorbing and nonadsorbing surfaces, J. Rheol. **46**, 831–862 (2002). 10.1122/1.1485279
8. D. E. Smith, H. P. Babcock and S. Chu, Single-Polymer dynamics in steady shear flow, Science **283**, 1724–1727 (1999). 10.1126/science.283.5408.1724
9. A. W. Vreman and J. G. M. Kuerten, Comparision of direct numerical simulation databases of turbulent channel flow at Re = 180, Phys. Fluids **26**, 015102 (2014). 10.1063/1.4861064

10. M. Lee and R. D. Moser, Extreme-scale motions in turbulent plane couette flows, J. Fluid Mech. **842**, 128–145 (2018). 10.1017/jfm.2018.131
11. J. Gregory and S. Barany, Adsorption and Flocculation by Polymers and Polymer Mixtures, Adv. Colloid Interface Sci. **169**, 1−12 (2011). 10.1016/j.cis.2011.06.004
12. V. Vajihinejad and J. B. P. Soares, Monitoring polymer flocculation in oil sand tailings: a population balance model appraoch, Chem. Eng. J. **346**, 447−457 (2018). 10.1016/j.cej.2018.04.039
13. P. Jarvis, B. Jefferson, J. Gregory and S. A Parsons, A review of floc strength and breakage, Water Res. **39**, 3121−3137 (2005). 10.1016/j.watres.2005.05.022